A Bispecific, Tetravalent Antibody Targeting Inflammatory and Pruritogenic Pathways in Atopic Dermatitis

Julia Tietz[1], Tea Gunde[1], Stefan Warmuth[1], Christopher Weinert[1], Matthias Brock[1], Alexandre Simonin[1], Christian Hess[1], Maria Johansson[1], Fabio Spiga[1], Simone Muntwiler[1], Belinda Wickihalder[1], Dana Mahler[1], Dania Diem[1], Julia Zeberer[1], Robin Heiz[1], Naomi Flückiger[1], Noriko Shiraishi[2], Yoshihide Miyake[2], Nobuaki Takahashi[2], Markus Fehrholz[3], Marta Bertolini[3], Peter Lichtlen[1], David Urech[1] and Daniel Snell[1]

Inhibition of IL-4/IL-13 signaling has dramatically improved the treatment of atopic dermatitis (AD). However, in many patients, clinical responses are slow to develop and remain modest. Indeed, some symptoms of AD are dependent on IL-31, which is only partially reduced by IL-4/IL-13 inhibition. Thus, there is an unmet need for AD treatments that concomitantly block IL-4/IL-13 and IL-31 pathways. We engineered NM26-2198, a bispecific tetravalent antibody designed to accomplish this task. In reporter cell lines, NM26-2198 concomitantly inhibited IL-4/IL-13 and IL-31 signaling with a potency comparable with that of the combination of an anti–IL-4Rα antibody (dupilumab) and an anti–IL-31 antibody (BMS-981164). In human PBMCs, NM26-2198 inhibited IL-4–induced upregulation of CD23, demonstrating functional binding to FcγRII (CD32). NM26-2198 also inhibited the secretion of the AD biomarker thymus and activation-regulated chemokine (TARC) in blood samples from healthy human donors. In male cynomolgus monkeys, NM26-2198 exhibited favorable pharmacokinetics and significantly inhibited IL-31–induced scratching at a dose of 30 mg/kg. In a repeat-dose, good laboratory practice toxicology study in cynomolgus monkeys, no adverse effects of NM26-2198 were observed at a weekly dose of 125 mg/kg. Together, these results justify the clinical investigation of NM26-2198 as a treatment for moderate-to-severe AD.

Keywords: Atopic dermatitis, Cytokines, Inflammatory skin diseases, Pruritus

JID Innovations (2024);**4:**100258 doi:10.1016/j.xjidi.2024.100258

INTRODUCTION

Atopic dermatitis (AD) is a T helper 2 cell–driven chronic skin disease characterized by systemic inflammation, barrier dysfunction, and persistent itch (Bieber, 2010; Moyle et al, 2019). Patients with moderate-to-severe AD experience intense pruritus, infectious complications, systemic comorbidities, mental health disorders, and impaired QOL (Moyle et al, 2019). The first biologic agent approved for treatment of moderate-to-severe AD, dupilumab, improved composite measures of AD severity in phase III trials (Blauvelt et al, 2017; de Bruin-Weller et al, 2018; Simpson et al, 2016). Eczema severity and area were reduced by 75% in about half of dupilumab-treated patients within 16 weeks (Simpson et al, 2016). Dupilumab also improved scores for secondary outcomes related to pruritus, but pruritus improvements were incomplete (about 50% mean improvement after 16 weeks) and typically exhibited slow onset (~20% mean improvement after 2 weeks) (Blauvelt et al, 2021, 2017; de Bruin-Weller et al, 2018; Simpson et al, 2016). Pruritus is one of the most troubling symptoms for patients with AD because it induces the itch–scratch cycle, which reinforces skin inflammation, and because it is strongly linked to impaired QOL (Moyle et al, 2019). Thus, treatment of moderate-to-severe AD may require adjunctive therapies directly targeting pruritus. Furthermore, because scratching is a major contributor to barrier dysfunction and disease persistence (Bieber, 2010; Bieber et al, 2021; Guttman-Yassky et al, 2018; Trier and Kim, 2018; Wahlgren, 1999), more rapid and complete alleviation of itch may improve the rapidity and magnitude of treatment efficacy.

Dupilumab blocks IL-4Rα, thereby inhibiting both IL-4 and IL-13 signaling, owing to the requirement for IL-13Rα1 to heterodimerize with IL-4Rα (Bitton et al, 2020; Moyle et al, 2019). Dupilumab has helped to establish the central role of these cytokines in the pathogenesis of AD (Guttman-Yassky et al, 2018; Trier and Kim, 2018; Werfel et al, 2016). Studies of selective IL-13 inhibitors further support this role (Gonçalves et al, 2021). Nevertheless, pruritus in AD is dependent on another T helper 2–derived cytokine, IL-31,

[1]Numab Therapeutics AG, Zürich, Switzerland; [2]Kaken Pharmaceutical, Tokyo, Japan; and [3]Monasterium Laboratory GmbH, Münster, Germany

Correspondence: Daniel Snell, Numab Therapeutics AG, Bachtobelstrasse 5, CH-8810 Horgen, Zürich, Switzerland. E-mail: d.snell@numab.com

Abbreviations: AD, atopic dermatitis; CO_2, carbon dioxide; IV, intravenous; SPR, surface plasmon resonance; SC, subcutaneous; STAT, signal transducer and activator of transcription; TARC, thymus and activation-regulated chemokine

Received 3 October 2023; revised 21 December 2023; accepted 26 December 2023; accepted manuscript published online XXX; corrected proof published online XXX

Cite this article as: JID Innovations 2024;4:100258

© 2024 The Authors. Published by Elsevier Inc. on behalf of the Society for Investigative Dermatology. This is an open access article under the CC BY-NC-ND license (http://creativecommons.org/licenses/by-nc-nd/4.0/).

which directly stimulates cutaneous nerve endings, macrophages, and keratinocytes (Cevikbas et al, 2014; Datsi et al, 2021; Dillon et al, 2004; Takamori et al, 2018; Trier and Kim, 2018). Although dupilumab treatment can reduce the expression of IL-31 in the skin (Guttman-Yassky et al, 2019), dupilumab does not directly reduce IL-31 serum levels in patients with AD (Kishi et al, 2023). Clinical studies have shown that a mAb targeting IL-31RA, nemolizumab, partially reduces pruritus and inflammation in patients with moderate-to-severe AD or prurigo nodularis (Ruzicka et al, 2017; Silverberg et al, 2020; Ständer et al, 2020). Thus, direct inhibition of IL-31 is a promising adjunctive strategy for more rapid and complete alleviation of itch in patients with AD. However, combination therapy with dupilumab and nemolizumab is likely to be expensive, clinically challenging, and burdensome for patients. Furthermore, as of this writing, nemolizumab is not approved for clinical use outside Japan. JAK inhibitors are available but have serious safety concerns (Blauvelt et al, 2021; Reich et al, 2022). Therefore, there is a strong unmet need for rapidly acting, efficacious, safe, and clinically convenient treatment options targeting multiple cytokine pathways involved in AD.

To address this unmet need, we have developed NM26-2198, an antibody-based therapeutic that concomitantly antagonizes cytokine pathways central to inflammatory immune activation in AD (IL-4 and IL-13) and those central to atopic itch (IL-31). NM26-2198 is a bispecific, tetravalent IgG4 single-chain variable fragment molecule targeting IL-4Rα and IL-31 with a molecular weight of 202 kDa. In this report, we describe the biochemical properties and in vitro and in vivo functional activities of NM26-2198. These studies support the clinical development of NM26-2198 for treatment of moderate-to-severe AD.

RESULTS AND DISCUSSION

IL-4, IL-13, and IL-31 co-operatively change the expression of genes related to AD in human skin samples

AD is associated with upregulation and downregulation of hundreds of genes, including differential effects in lesional versus nonlesional skin, as well as changes in the expression of genes involved in systemic inflammatory and immune responses (Ewald et al, 2015). Transcriptome profiling may be useful for predicting therapeutic responses (Ewald et al, 2015); indeed, changes in gene expression patterns in dupilumab-treated patients with AD were correlated with pathologic and clinical improvements (Guttman-Yassky et al, 2019). Thus, we used gene expression profiling to explore the biologic rationale for combining IL-4/IL-13 inhibition with IL-31 inhibition as a potential treatment for AD. Normal human skin biopsy samples from 3 healthy human donors were treated ex vivo with IL-4, IL-13, and IL-31 alone or in combination. IL-4 and IL-13 treatment induced significant changes in gene expression in these tissues, but IL-31 alone had limited effects (Figure 1). However, the combination of all 3 cytokines induced significantly more changes in gene expression than either IL-4/IL-13 or IL-31 alone. In particular, expression of genes related to neurological and keratinocyte function was altered (Figure 1c). Expression of genes related to inflammatory pathways was also altered during treatment with all 3 cytokines, suggesting an inflammatory role for IL-31 in addition to its role in neurological signaling. These data are consistent with the effects of nemolizumab treatment on neuronal and inflammatory markers in patients with prurigo nodularis (Deng et al, 2023).

These results provide initial evidence of a biologic rationale for combining inhibitors of IL-4/IL-13 and IL-31 cytokine pathways to treat AD, consistent with observations from clinical trials described in the introduction. The results are also consistent with those of a recent study in 12 patients with AD, which showed that dupilumab treatment significantly reduced some biomarkers of AD (serum levels of IgE, IL-22, and thymus and activation-regulated chemokine [TARC]) but did not affect the number of intraepidermal nerve fibers, which are associated with itch severity and positively correlated with IL-31 levels (Kishi et al, 2023).

A tetravalent, bispecific IgG4 targeting AD cytokine pathways

Because of the biological and clinical rationale for concomitant inhibition of IL-4/IL-13 and IL-31 pathways as a treatment for AD, we developed an antibody-based molecule that simultaneously targets both pathways. NM26-2198 is a recombinant, tetravalent, bispecific IgG4 in which λ-capped anti−IL-31 single-chain variable fragments are fused to the C-termini of both anti−IL-4Rα IgG4 heavy chains through flexible peptide $(Gly_4–Ser)_2$ linkers (Figure 2) (Coloma and Morrison, 1997; Egan et al, 2017). An IgG4 backbone was chosen because of its reduced effector function (Davies and Sutton, 2015). To prevent Fab arm exchange, the core-hinge region of the heavy chain contains an S228P mutation (Silva et al, 2015).

The anti−IL-4Rα and anti−IL-31 sequences were originally derived from rabbit mAbs. The complementarity-determining regions were grafted onto human variable domain acceptor frameworks. The anti−IL-31 framework was engineered from human consensus and germline sequences for favorable stability and solubility using λ-cap technology (Egan et al, 2017). The single-chain variable fragments were then further engineered to improve stability for use at high concentrations.

NM26-2198 exhibits high-affinity target binding and potent and concomitant inhibition of IL-4R and IL-31 signaling

Binding of NM26-2198 to recombinant human IL-4Rα extracellular domain and IL-31 was assessed by surface plasmon resonance (SPR) (Figure 3a and b). Mean (±SD) equilibrium dissociation constants were 209 ± 68 pM for human IL-4Rα (n = 3) and 193 ± 88 pM for human IL-31 (n = 3). Concomitant binding to human IL-4R and human IL-31 was also demonstrated by SPR (Figure 3c).

We then studied the ability of NM26-2198 to inhibit either of its target pathways (IL-4/IL-13, IL-31) alone or in the presence of excess amounts of the other target. Figure 3d and e show that NM26-2198 inhibited IL-4− and IL-13−induced secretion of a signal transducer and activator of transcription 6 (STAT6) reporter gene product in HEK-Blue cells with a potency comparable with that of dupilumab. The presence of an excess concentration of IL-31 (9.9 nM) had no effect on NM26-2198 inhibition of IL-4 or IL-13 signaling. Similarly, NM26-2198 inhibited IL-31−induced production of active beta-galactosidase in an osteosarcoma cell line (PathHunter U2OS cells) with a potency similar to that of the reference

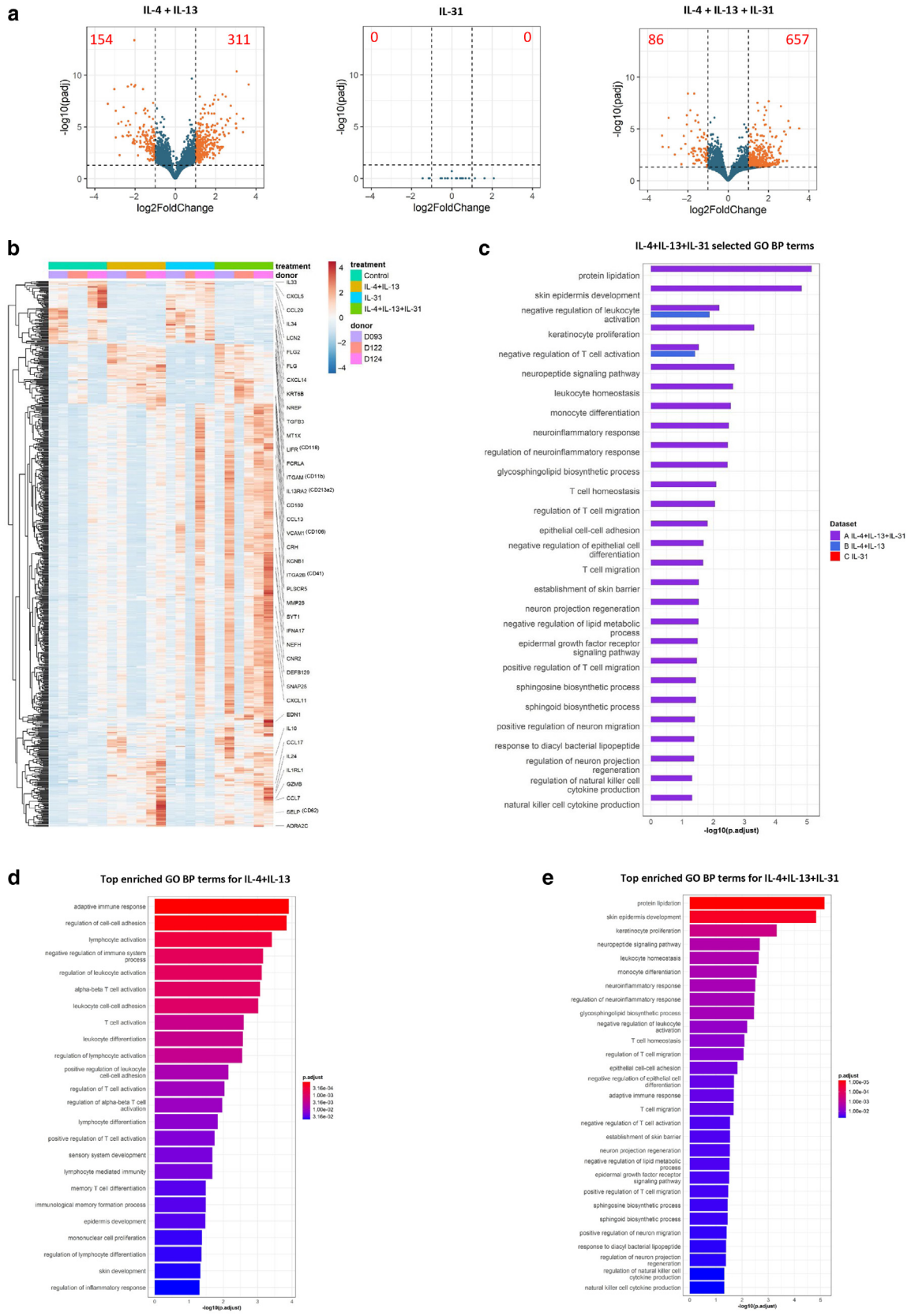

Figure 1. RNA-seq analysis of healthy human skin biopsies from 3 donors treated with IL-4, IL-13, and IL-31 at 50 ng/ml for 72 h. **(a)** Volcano plots showing genes whose expression was significantly altered (red) by IL-4 + IL-13 (left), IL-31 (middle), and IL-4 + IL-13 + IL-31 (right) treatments. **(b)** Heatmap showing relative expression of specific genes according to treatment condition and donor based on row Z-scores of all samples in the study, of which *FLG, FLG2, IL-24, CXCL-11, IL13Ra2, IL-33, LCN2, K6B, GZMB, CCL17,* and *CCL13* are known to play an important role in AD. Other important genes known to play a role in inflammatory and neural processes, keratinocytes, and/or barrier function are also highlighted on the right. **(c)** Bar plot showing changes in expression

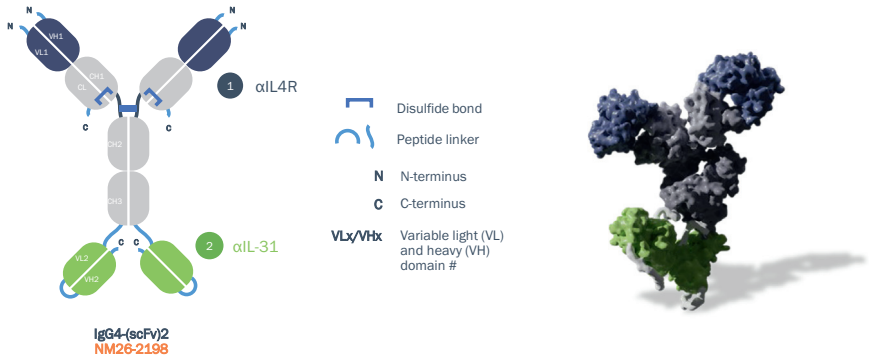

Figure 2. Schematic depiction (left) and structural model (right) of NM26-2198. The structural model was prepared using BIOVIA Discovery Studio software.

anti−IL-31 antibody BMS-981164. Inhibition by NM26-2198 was unaffected by the addition of excess IL-4Rα (Figure 3f).

To test whether NM26-2198 can concomitantly inhibit IL-4/IL-13 signaling and IL-31 signaling, we used human bronchial epithelial cells (BEAS-2B cells), which express the subunits of type I and type II IL-4 receptors (IL-4Rα, γcommon, and IL-13R α1) as well as subunits of the IL-31 receptor (IL-31RA and OSMRβ) (Ip et al, 2007; Yamamoto et al, 2004). Cells were incubated for 24 hours in control conditions or in the presence of various combinations of IL-4, IL-31, dupilumab, the anti−IL-31 antibody BMS-981164, and NM26-2198. As shown in Figure 3g, IL-4 and IL-31 each stimulated the release of CCL2, and incubation with both cytokines induced additive effects. Dupilumab and BMS-981164 each inhibited IL-4/IL-31−induced CCL2 secretion, and incubation with both antibodies exerted further antagonism. NM26-2198 antagonized CCL2 secretion at least as effectively as the combination of dupilumab and BMS-981164. Figure 3h shows dose−response curves for inhibition of IL-4/IL-31−induced CCL2 release by NM26-2198 or the combination of dupilumab and BMS-981164. Considered together, the results shown in Figure 3 demonstrate that NM26-2198 binds to both IL-4Rα and IL-31 independently and concomitantly, and it inhibits signaling through both pathways with a potency comparable with that of the combination of dupilumab and BMS-981164.

NM26-2198 potently inhibits IL-4−induced CD23 upregulation in PBMCs and TARC secretion in whole blood

One of the hallmarks of IL-4− and IL-13−induced immune responses is upregulation of CD23 (the low-affinity IgE receptor, FcεRII) on monocytes and B cells (Defrance et al, 1994; McCormick and Heller, 2015; Moyle et al, 2019). Anti−IL-4Rα antibodies have been shown to inhibit IL-4−induced CD23 upregulation, but their potency depends on the characteristics of antibody binding to FcγRII (CD32) (Zhao et al, 2019). Because NM26-2198 has an IgG4 isotype Fc moiety and has anti−IL-31 single-chain variable fragments attached to its C termini, it was important to assess its potency for inhibition of CD23 upregulation. We studied the effects of NM26-2198 on IL-4−induced CD23 expression in monocytes and B cells in PBMCs from healthy human donors. Incubation of PBMCs with IL-4 for 48 hours upregulated the expression of CD23 in monocytes, naïve B cells, and memory B cells, and this effect was inhibited by NM26-2198 in each cell type in a dose-dependent manner (Figure 4a−c). The half-maximal inhibitory concentration for NM26-2198 was comparable with that of dupilumab, which is also an IgG4. An Fc-silenced version of NM26-2198 (PRO2142) demonstrated a significant decrease in activity in this assay, particularly in monocytes, consistent with previous studies showing that Fc binding to FcγRII is essential for inhibition of IL-4−induced upregulation of CD23 in immune cells (Zhao et al, 2019). These experiments demonstrate that NM26-2198 retained FcγRII binding. NM26-2198 induced no detectable antibody-dependent cell-mediated cytotoxicity using Ramos B cells as target cells and human PBMCs as effector cells. Similarly, NM26-2198 did not induce complement-dependent cytotoxicity in Ramos B cells in the presence of human complement. Rituximab used as positive control showed potent activity in both assays (data not shown).

Another hallmark of AD and IL-4− and IL-13−induced immune responses is increased serum concentrations of the T helper 2 chemokine TARC (Hijnen et al, 2004; Jahnz-Rozyk et al, 2005; Kakinuma et al, 2001). Figure 4d−f shows TARC levels in whole human EDTA-anticoagulated blood from 3 healthy donors after 24 hours of incubation with IL-4 and the indicated concentrations of NM26-2198 or dupilumab. Both NM26-2198 and dupilumab inhibited TARC secretion, but their relative potency varied across the 3 donors. The half-maximal inhibitory concentration for inhibition of IL-4−induced TARC secretion by NM26-2198 ranged from 328 to 490 pM and averaged 409 ± 81.1 pM. Inhibition of IL-13−induced TARC secretion by NM26-2198 had a similar potency (286 ± 142 pM, data not shown), which is important because of evidence that IL-13 has a strong role in AD pathology (Lytvyn and Gooderham, 2023; Tazawa et al, 2004; Tsoi et al, 2019; Zhang et al, 2022). These results are consistent with clinical trial results in which dupilumab treatment reduced serum TARC levels in adult patients with AD (Guttman-Yassky et al, 2019) and suggest that NM26-2198 may have a similar effect in patients.

(log-transformed adjusted *P*-values) of gene clusters associated with selected gene ontology biological processes terms after treatment with the indicated ILs. There was no enrichment of the shown terms for IL-31. **(d, e)** Bar plots showing top enriched gene ontology biological processes terms after treatment with cytokines. AD, atopic dermatitis; h, hour; K6B, keratin 6B; RNA-seq, RNA sequencing.

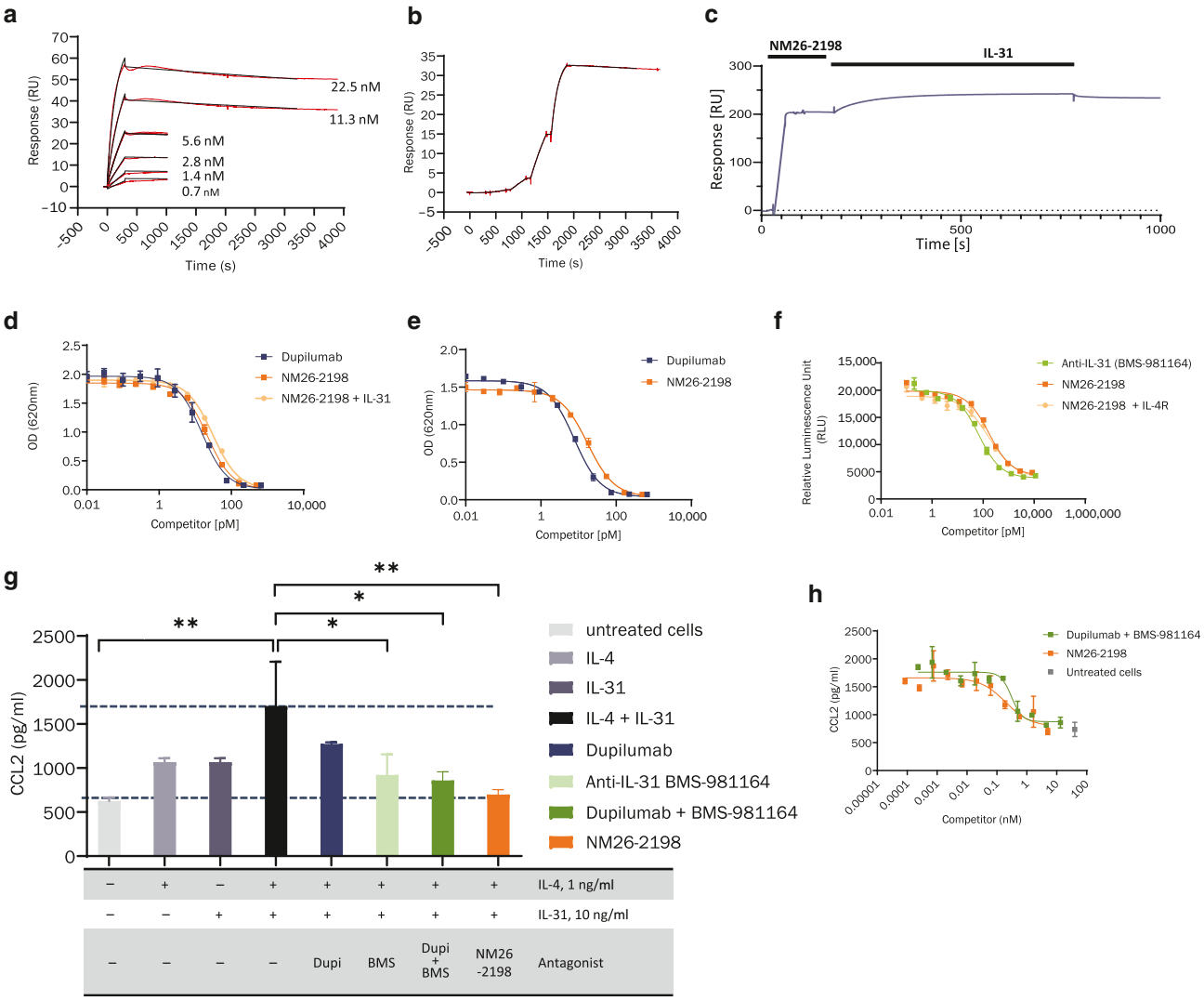

Figure 3. NM26-2198 binding kinetics and inhibition of cell signaling. **(a)** SPR sensorgrams of NM26-2198 binding to IL-4Ra in multicycle kinetic mode. **(b)** SPR sensorgram of NM26-2198 binding to IL-31 in single-cycle kinetic mode. Colored lines represent the experimental data, and black lines show the fit of a 1:1 interaction model. **(c)** SPR sensorgram showing concomitant binding of NM26-2198 to human IL-4R (immobilized) and IL-31. **(d)** SEAP concentration in the supernatant of HEK-Blue IL-4/IL-13 STAT6 reporter gene cells measured using the QUANTI-Blue colorimetric assay and reported as mean (SD) optical density. Cells were cultured in the presence of IL-4 (0.05 ng/ml, 23.8 pM) for 24 hours to induce SEAP secretion. Culture media also contained the indicated concentrations of dupilumab or NM26-2198 in the presence or absence of excess IL-31 (9.9 nM). **(e)** Mean (SD) SEAP concentrations in similar experiments as **d** except that cells were cultured in the presence of IL-13 (0.3 ng/ml, 23.8 pM) instead of IL-4. **(f)** Mean (SD) chemiluminescence of engineered U2OS cells indicating IL-31—induced heterodimerization of IL-31RA and OSMR after 6 hours incubation with IL-31 (10 ng/ml, 0.63 nM) and the indicated concentrations of BMS-981164 or NM26-2198 in the presence or absence of excess IL-4R extracellular domain (50 nM). **(g)** Mean (SD) CCL2 concentrations in the supernatant of cultured BEAS-2B cells after 24-hour incubation with the indicated ILs and antagonists. Antagonist concentrations were 1 mg/ml (5 nM dupilumab and 5 nM BMS-981164, 6.7 nM NM26-2198). Results are mean (SD) of 1 independent experiment. *P*-values are based on Dunnett's test performed after an overall $P = .012$ by ANOVA. * $P < .05$ and ** $P < .01$. **(h)** CCL2 concentrations in supernatant of BEAS-2B cells after 24-hour incubation with IL-4 (1 ng/ml) and IL-31 (10 ng/ml) and the indicated concentrations of dupilumab + BMS-981164 or NM26-2198. **a** and **b** are representative of 3 experiments, and **c**—**h** correspond to 1 experiment. Duplicate wells were used for experiments shown in **d**—**h**. OSMR, oncostatin M receptor; SEAP, secreted embryonic alkaline phosphatase; SPR, surface plasmon resonance; STAT6, signal transducer and activator of transcription 6.

NM26-2198 exhibits a long serum half-life in cynomolgus monkeys and abrogates itching symptoms triggered by IL-31

In SPR assays, NM26-2198 exhibited binding kinetics and affinities for cynomolgus monkey IL-4Rα (equilibrium dissociation constant = 144 ± 49 pM, n = 3) and IL-31 (equilibrium dissociation constant = 103 ± 14 pM, n = 3) similar to those for human targets (mean equilibrium dissociation constant = 209 pM for IL-4Rα and 193 pM for IL-31).

The pharmacokinetics of single doses of NM26-2198, administered by intravenous (IV) or subcutaneous (SC) injection, were studied in cynomolgus monkeys. Mean serum drug levels at designated times after administration of 3 dose levels are shown in Figure 5a for IV administration (and 5 mg/kg SC) and Figure 5b for higher-dose SC administration. NM26-2198 serum concentrations increased with increasing dose levels for both IV and SC routes of administration. The mean serum half-life of NM26-2198 was 7—10 days across

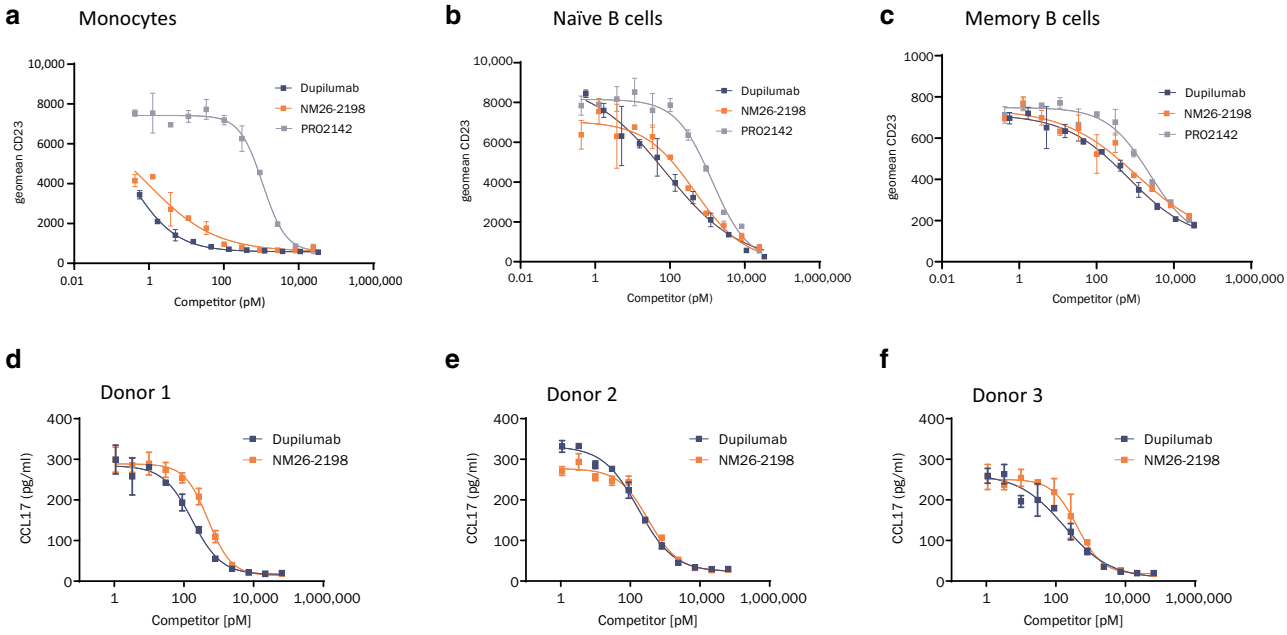

Figure 4. NM26-2198 inhibition of IL-4—induced CD23 expression in human monocytes and B cells and of IL-4—induced TARC secretion in whole human blood. **(a—c)** Geometric mean CD23 expression in **(a)** monocytes, **(b)** naïve B cells, or **(c)** memory B cells measured by flow cytometry after 48-hour incubation of PBMCs with IL-4 (2 ng/ml) and the indicated concentrations of NM26-2198, its IgG1-Fc silenced version PRO2142, or dupilumab. **(d—f)** Secretion of TARC (CCL17) in specimens of whole human blood from 3 donors after 24-hour incubation with IL-4 (1 ng/ml) and the indicated concentrations of dupilumab or NM26-2198. Secretion was quantified by ELISA, and the values shown are means (SD) of duplicate measurements at each concentration. TARC, thymus and activation-regulated chemokine.

doses above 1 mg/kg. The faster clearance of the 1 mg/kg IV dose is likely due to target-mediated drug disposition to IL-4Rα.

We then studied the effects of NM26-2198 on scratching symptoms in cynomolgus monkeys. Male monkeys not exhibiting strong baseline scratching symptoms were randomized into 5 treatment groups: vehicle or 1 of 4 doses of NM26-2198 (0.03, 0.3, 3, and 30 mg/kg). Between 28 and 18 days before treatment, monkeys received an IV injection of cynomolgus IL-31 (1 μg/kg) and were grouped according to this baseline treatment (Figure 5c). Video recordings of monkey behavior were used to monitor scratching events for 1 hour before injection and for 3 hours after injection. On day 1, monkeys received a SC injection of their randomly allocated treatment. On day 3, injection of cynomolgus IL-31 and video recording procedures were repeated to evaluate how treatment affected the number of scratching events. Figure 5d shows the mean time-normalized number of scratching events in each of the treatment groups. Monkeys in the 3 mg/kg and 30 mg/kg NM26-2198 groups exhibited lower mean scratching frequency than those in the vehicle-treated group, and this effect was statistically significant for the 30 mg/kg group (overall $P = .003$ by ANOVA; $P = .017$ for 30 mg/kg group vs vehicle group by Dunnett's test). It should be noted that this is not an AD model but only reflective of inhibition of IL-31—induced scratching behavior.

Good laboratory practice toxicology in cynomolgus monkey

A formal, 4-week, repeat-dose good laboratory practice toxicology study was conducted in cynomolgus monkeys, in which monkeys received 5 weekly doses of NM26-2198 through either SC route (5, 25, or 125 mg/kg) or IV route (125 mg/kg). No treatment-related findings were observed. Monkeys exhibited no evidence of gross pathological changes; histopathological changes; injection site inflammation; ophthalmologic changes; or cardiovascular, respiratory, or neurologic changes during the 4-week study period. On the basis of these results, the no-observed effect level for NM26-2198 in cynomolgus monkey is 125 mg/kg, well above the dose level required for efficacy shown in the preceding experiment. Considered together, the results presented in this paper justify the clinical investigation of NM26-2198 as a treatment for AD, and a phase I clinical study is ongoing (NCT05859724).

MATERIALS AND METHODS

Reference antibodies and selected reagents

Dupilumab was produced by Evitria AG from published sequence data (CAS number 1190264-60-8) or purchased at the pharmacy (Dupixent, Sanofi). BMS-981164 was produced by Evitria AG on the basis of the sequence published in patents US8470979B2 and WO09071696. NM26-2198 was manufactured by Numab Therapeutics AG. CCL2 antibodies and antibodies for PBMC staining were acquired at Biolegend (San Diego, CA). IL-4, IL-13, and IL-31 were purchased from PeproTech (Rocky Hill, NJ).

RNA-sequencing analysis of human skin samples

Skin punch tissue samples were collected from healthy human donors and cultured at 37 °C (5% carbon dioxide [CO_2]) in a mixture (1:1) of RPMI and William's E media (Gibco, Thermo Fisher Scientific, Waltham, MA) (Gherardini et al, 2020) with 10 ng/ml hydrocortisone (Sigma-Aldrich, Merck, Burlington, MA), 10 μg/ml insulin (Sigma-Aldrich, Buchs, Switzerland), 2 mM L-glutamine (Sigma-

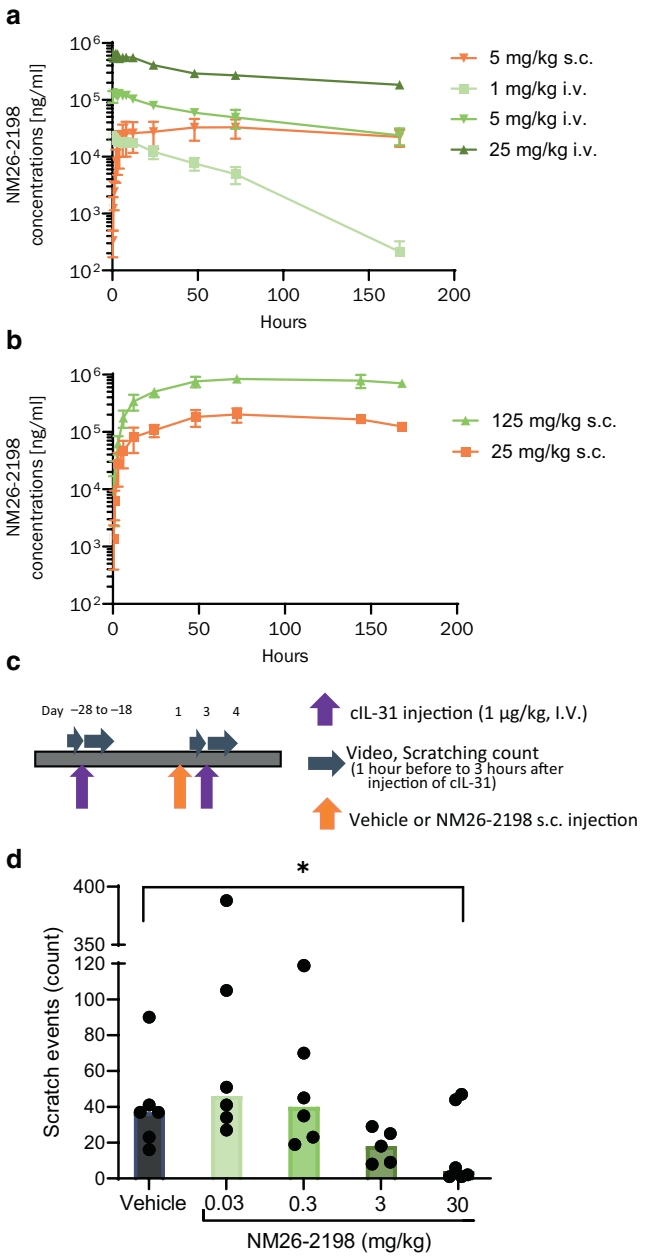

Figure 5. NM26-2198 pharmacokinetics and inhibition of IL-31–induced scratching in cynomolgus monkeys. **(a, b)** Mean (SD) serum drug levels at indicated times after intravenous (green) or subcutaneous (orange) administration of single doses of NM26-2198 to cynomolgus monkeys (n = 6 per treatment condition, except n = 5 for 3 mg/kg group). **(c)** Treatment timeline of scratching study as described in the text. Monkeys were grouped according to baseline treatment (day −28 to day −18). **(d)** Number of scratching events during 3 hours after IL-31 injection minus 3× the number of scratching events during the 1 hour preceding IL-31 injection. Filled circles indicate results for each monkey; bars indicate the mean for each treatment condition. *$P < .05$ (0.017) for monkeys treated with 30 mg/kg versus vehicle on the basis of Dunnett's test performed after an overall $P = .003$ by ANOVA.

Aldrich), and 1% penicillin/streptomycin (Gibco). Treatment with IL-4, IL-13 (Keren et al, 2023), and IL-31 was performed at initiation of culture and at 48 hours. Samples were collected at 72 hours for RNA extraction.

RNA sequencing was performed on a NovaSeq 6000 using a 2 × 100 bp read length with an output of approximately 30 M clusters (6 Gb) per sample. Trimmed raw reads were aligned to a modified HG19 using STAR (version 2.7.3) (Dobin et al, 2013). Pseudoautosomal regions were masked on chromosome Y (chrY:10001-2649520, chrY:59034050- 59363566). Normalized counts were calculated with DESeq2 (version 1.40.1). Volcano plots, heatmap, and bar plots were generated with R (version 4.3.0) using the ggplot2 package (version 3.4.2) and pheatmap (version 1.0.12). Gene set enrichment analysis was performed using clusterProfiler (version 4.9.0) and DOSE (version 3.26.1) (Yu et al, 2015). Volcano plots are representative of the results of all 3 donors.

Binding affinity and concomitant binding by SPR

SPR analysis was performed on a T200 Biacore instrument (Cytiva, Uppsala, Sweden). For IL-4Rα, NM26-2198 was captured on a CM5 sensorchip (Cytiva) using an IgG-Fc antibody (Human Antibody Capture Kit, Cytiva). A titration series of IL-4Rα extracellular domain-his-tag (Sino Biological, Bejing, China) was injected in saline 4-(2-hydroxyethyl)-1-piperazineethanesulfonic acid buffer (0.05% Tween-20, pH 7.5). The sensor chip was regenerated with magnesium chloride. For IL-31, NM26-2198 was injected over a CM5 sensor chip with IL-4R-Fc Tag (R&D Systems, Freiburg, Germany), followed by IL-31. Concomitant binding to IL-4R and Il-31 was assessed using a CM5 sensorchip with IL-4R-Fc immobilized, followed by a sequential flow of NM26-2198 and IL-31. Binding to monkey IL-4Rα and IL-31 was measured using IL-4Rα extracellular domain-His (Acro Biosystems, Newark, DE) and IL-31-His (Sino Biological) of cynomolgus monkey. Kinetics were calculated with Biacore evaluation software (version 3.2, Cytiva, 1:1 Langmuir model).

Inhibition of IL-4 and IL-13 signaling

Assays used HEK-Blue IL-4/IL-13 STAT6 cells (hkb-il413, InvivoGen, Toulouse, France), producing secreted embryonic alkaline phosphatase through the STAT6 pathway in response to IL-4 or IL-13. A total of 50,000 cells per well were seeded into 96-well plates in DMEM high glucose with 10% heat-inactivated fetal calf serum (Sigma-Aldrich). NM26-2198 or dupilumab were added with human IL-4 or human IL-13. After 24 hours of incubation at 37 °C and 5% CO_2, supernatants were transferred to a new plate, and secreted embryonic alkaline phosphatase was quantified using QUANTI-Blue (InvivoGen) with a Tecan plate reader (Infinite M-Plex, Grödig, Austria). Inhibition curves were fitted using a 4-parameter logistic regression model in GraphPad prism 9.1.0.

Inhibition of IL-31 signaling

Assays used PathHunter U2OS IL31RA/OSMRβ dimerization cell line (DiscoverX, Celle-l'Evescault, France), producing a chemiluminescent signal upon ligand-induced dimerization of OSMRβ/IL31RA. A total of 10,000 cells per well were seeded into 96-well plates in Assay Complete Cell Plating 5 Reagent overnight (DiscoverX) before addition of NM26-2198 or BMS-981164 with IL-31. After 6 hours (37 °C, 5% CO_2), a detection solution was added for an hour (Path Hunter Flash Detection Kit, DiscoverX), and luminescence was measured.

Simultaneous inhibition of IL-4 and IL-31 signaling

Assays used BEAS-2B cells (LCR-9609, ATCC, Manassas, VA), in which CCL2 release is increased in response to additive stimulation by IL-31 and IL-4. A total of 25,000 cells per well were seeded into 96-well plates in 100 µl DMEM/Nutrient Mixture F-12 Ham (Sigma-Aldrich, Irvine, United Kingdom) with 10% heat heat-inactivated fetal calf serum (Sigma-Aldrich) and incubated overnight (37 °C,

5% CO_2). After 2 washing steps, IL-4 and/or IL-31 were added with or without NM26-2198 or a combination of dupilumab and BMS-981164. Supernatants were collected after 24 hours.

For quantification of CCL2 by ELISA, 96-well plates were coated with 1 μg/ml of a mouse CCL2 antibody in PBS. Plates were blocked with PBS (0.2% Tween,1% BSA). Serial dilutions of CCL2 in Low Cross buffer (Candor, Wangen, Germany) and supernatants were added. CCL2 was detected with 0.25 mg/ml of a biotinylated hamster CCL2 antibody and with 100 ng/ml streptavidin-horse radish peroxidase (Stereospecific Detection Technologies, Baesweiler, Germany). SureBlue Reserve was added (SeraCare, Milford, MA) and then hydrogen chloride. The optical density was read at 450 nm.

Inhibition of IL-4 induced CD23 expression on human monocytes and naïve and memory B cells

Human PBMCs were isolated from fresh whole blood of healthy donors according to an adapted Leucosep protocol using tubes with integrated porous barrier and gradient density centrifugation, first at 800*g* without brakes and then at 300*g* with brakes. A total of 400,000 PBMCs were seeded per well into a 96-well plate in 100 μl of medium (RPMI, Irvine Scientific;10% heat-inactivated fetal calf serum, Sigma-Aldrich). NM26-2198 or dupilumab was added with human IL-4. After 48 hours of incubation (37 °C, 5% CO_2), FcR blocking solution (Human TruStain FcX, BioLegend) was added, and PBMCs were stained for flow cytometry analysis (Novocyte, AECA Biosciences, San Diego, CA) using mouse anti-human CD14-PerCP/Cy5.5, CD19-phycoerythrin, CD27-FITC, and CD23-allophycocyanin antibodies. The geometric mean of gated CD23 monocytes, CD23 naïve, and memory B cells was used for evaluation.

Inhibition of IL-4–induced TARC secretion in human whole blood

Human peripheral blood was collected in sterile tubes containing EDTA. A total of 160 μl per well of serial dilutions of NM26-2198 or dupilumab was added to a 96-well plate with IL-4 in IMDM (Thermo Fisher Scientific, Paisley, United Kingdom; containing 1% heat-inactivated fetal calf serum). After addition of 40 μl whole blood per well, plates were incubated for 24 hours (37 °C, 5% CO_2) and centrifuged for 10 minutes at 1000*g*. Supernatants were collected and frozen at −20 °C. TARC was quantified using the human TARC/CCL17 DuoSet ELISA Kit (R&D Systems, Minneapolis, MN) according to kit instructions.

Studies in cynomolgus monkey

Pharmacokinetic assessment was performed in male cynomolgus monkeys of African (Mauritius) origin at Charles River Laboratories. Serum levels of NM26-2198 were determined using a validated pharmacokinetics ELISA. An itch study was performed at Shin Nippon Biomedical Laboratories by administering a single dose (SC) of NM26-2198 to male cynomolgus monkeys. Forty-eight hours later, cynomolgus IL-31 was administered intravenously, and the frequency and duration of scratching behavior were evaluated.

Statistical analysis

Data are expressed as the mean ± SD of the mean. Differential expression was assessed using the Wald test within DESeq2, and false discovery rate was controlled using the Benjamin–Hochberg correction. For comparison of BEAS-2B assay results, ANOVA with pairwise comparisons with stimulated cells (IL-4 + IL-31) using posthoc Dunnett's test was performed assuming normal distribution of the sample (n = 2 per group). For analysis of the cynomolgus itch study, ANOVA with pairwise comparisons with vehicle using Dunnett's test of log-transformed values was performed after confirming normal distribution by Shapiro–Wilk test. The statistical tests were performed using GraphPad prism 9.1.0. For all tests, $P < .05$ was considered statistically significant.

ETHICS STATEMENT

All studies using cynomolgus macaques were in compliance with applicable animal welfare acts and were in accordance with local committees. The test facilities Charles River Laboratories and Shin Nippon Biomedical Laboratories are Association for Assessment and Accreditation of Laboratory Animal Care International accredited.

For studies using human blood, donors provided written informed consent. Blood samples were collected, anonymized, and used according to ethical approval from Blutspende Zurich (BASEC Nr. Req 2020-00983). All human skin samples were obtained after informed, written patient consent (all female) and ethics committee approval (Ethik-Kommission der Ärztekammer Westfalen-Lippe 2015-602-f-S; Ethik-Kommission Ärztekammer Berlin Eth-10/15).

DATA AVAILABILITY STATEMENT

To request data, please contact DS at Numab Therapeutics AG at d.snell@numab.com.

ORCIDs

Julia Tietz: http://orcid.org/0009-0006-5103-0842
Tea Gunde: http://orcid.org/0000-0002-9167-622X
Stefan Warmuth: http://orcid.org/0000-0001-6872-8805
Christopher Weinert: http://orcid.org/0000-0003-3313-9458
Matthias Brock: http://orcid.org/0000-0001-6445-0631
Alexandre Simonin: http://orcid.org/0009-0009-3022-8974
Christian Hess: http://orcid.org/0009-0006-4556-6288
Maria Johansson: http://orcid.org/0009-0001-3106-1629
Fabio Spiga: http://orcid.org/0000-0002-0541-3141
Simone Muntwiler: http://orcid.org/0009-0006-3231-4639
Belinda Wickihalder: http://orcid.org/0009-0003-1207-105X
Dana Mahler: http://orcid.org/0009-0003-2944-3040
Dania Diem: http://orcid.org/0009-0005-3215-8018
Julia Zeberer: http://orcid.org/0009-0001-6009-4163
Robin Heiz: http://orcid.org/0009-0008-7017-538X
Naomi Flückiger: http://orcid.org/0009-0004-3475-7543
Noriko Shiraishi: http://orcid.org/0009-0005-6206-424X
Yoshihide Miyake: http://orcid.org/0009-0007-7038-5670
Nobuaki Takahashi: http://orcid.org/0000-0001-8802-301X
Markus Fehrholz: http://orcid.org/0000-0003-2183-2415
Marta Bertolini: http://orcid.org/0000-0002-5927-6998
Peter Lichtlen: http://orcid.org/0009-0002-3441-0553
David Urech: http://orcid.org/0009-0003-2167-7440
Daniel Snell: http://orcid.org/0000-0003-0107-4821

CONFLICT OF INTEREST

The authors are employees of Numab Therapeutics AG. NS, YM, and NT are employees of Kaken Pharmaceutical. MB and MF are employees of Monasterium Laboratory - Skin & Hair Research Solutions GmbH. Research and manuscript preparation were supported by Numab Therapeutics AG.

ACKNOWLEDGMENTS

Scientific writing support was provided by Ken Scholz and funded by Numab Therapeutics AG.

AUTHOR CONTRIBUTIONS

Conceptualization: TG, DU, NS; Data curation: JT, DS, MF; Formal Analysis: AS, RH, NF, MS, BW, DD, DM, JZ, NG, MF, NT; Investigation: SW, CH, CW, MW, JT, FS, MB, DS, MB, MF, NT; Writing – Original Draft Preparation: JT; Writing – Review and Editing: JT, DS, TG, SW, PL, MB, FS, MF, NS, NT

REFERENCES

Bieber T. Atopic dermatitis. Ann Dermatol 2010;22:125–37.

Bieber T, Simpson EL, Silverberg JI, Thaçi D, Paul C, Pink AE, et al. Abrocitinib versus placebo or dupilumab for atopic dermatitis. N Engl J Med 2021;384:1101–12.

Bitton A, Avlas S, Reichman H, Itan M, Karo-Atar D, Azouz NP, et al. A key role for IL-13 signaling via the type 2 IL-4 receptor in experimental atopic dermatitis. Sci Immunol 2020;5:eaaw2938.

Blauvelt A, de Bruin-Weller M, Gooderham M, Cather JC, Weisman J, Pariser D, et al. Long-term management of moderate-to-severe atopic dermatitis with dupilumab and concomitant topical corticosteroids (Liberty AD Chronos): a 1-year, randomised, double-blinded, placebo-controlled, phase 3 trial. Lancet 2017;389:2287–303.

Blauvelt A, Teixeira HD, Simpson EL, Costanzo A, De Bruin-Weller M, Barbarot S, et al. Efficacy and safety of upadacitinib vs dupilumab in adults with moderate-to-severe atopic dermatitis: A randomized clinical trial. JAMA Dermatol 2021;157:1047–55.

Cevikbas F, Wang X, Akiyama T, Kempkes C, Savinko T, Antal A, et al. A sensory neuron-expressed IL-31 receptor mediates T helper cell-dependent itch: involvement of TRPV1 and TRPA1. J Allergy Clin Immunol 2014;133:448–60.

Coloma MJ, Morrison SL. Design and production of novel tetravalent bispecific antibodies. Nat Biotechnol 1997;15:159–63.

Datsi A, Steinhoff M, Ahmad F, Alam M, Buddenkotte J. Interleukin-31: the "itchy" cytokine in inflammation and therapy. Allergy 2021;76:2982–97.

Davies AM, Sutton BJ. Human IgG4: a structural perspective. Immunol Rev 2015;268:139–59.

de Bruin-Weller M, Thaçi D, Smith CH, Reich K, Cork MJ, Radin A, et al. Dupilumab with concomitant topical corticosteroid treatment in adults with atopic dermatitis with an inadequate response or intolerance to ciclosporin A or when this treatment is medically inadvisable: a placebo-controlled, randomized phase III clinical trial (Liberty AD CAFÉ). Br J Dermatol 2018;178:1083–101.

Defrance T, Carayon P, Billian G, Guillemot JC, Minty A, Caput D, et al. Interleukin 13 is a B cell stimulating factor. J Exp Med 1994;179:135–43.

Deng J, Liao V, Parthasarathy V, Cornman HL, Kambala A, Kwatra MM, et al. Modulation of neuroimmune and epithelial dysregulation in patients with moderate to severe prurigo nodularis treated with nemolizumab. JAMA Dermatol 2023;159:977–85.

Dillon SR, Sprecher C, Hammond A, Bilsborough J, Rosenfeld-Franklin M, Presnell SR, et al. Interleukin 31, a cytokine produced by activated T cells, induces dermatitis in mice. Nat Immunol 2004;5:752–60.

Dobin A, Davis CA, Schlesinger F, Drenkow J, Zaleski C, Jha S, et al. STAR: ultrafast universal RNA-seq aligner. Bioinformatics 2013;29:15–21.

Egan TJ, Diem D, Weldon R, Neumann T, Meyer S, Urech DM. Novel multispecific heterodimeric antibody format allowing modular assembly of variable domain fragments. mAbs 2017;9:68–84.

Ewald DA, Malajian D, Krueger JG, Workman CT, Wang T, Tian S, et al. Meta-analysis derived atopic dermatitis (MADAD) transcriptome defines a robust AD signature highlighting the involvement of atherosclerosis and lipid metabolism pathways. BMC Med Genomics 2015;8:60.

Gherardini J, Uchida Y, Hardman JA, Chéret J, Mace K, Bertolini M, et al. Tissue-resident macrophages can be generated de novo in adult human skin from resident progenitor cells during substance P-mediated neurogenic inflammation ex vivo. PLoS One 2020;15:e0227817.

Gonçalves F, Freitas E, Torres T. Selective IL-13 inhibitors for the treatment of atopic dermatitis. Drugs Context 2021;10. 2021-1-7.

Guttman-Yassky E, Bissonnette R, Ungar B, Suárez-Fariñas M, Ardeleanu M, Esaki H, et al. Dupilumab progressively improves systemic and cutaneous abnormalities in patients with atopic dermatitis. J Allergy Clin Immunol 2019;143:155–72.

Guttman-Yassky E, Krueger JG, Lebwohl MG. Systemic immune mechanisms in atopic dermatitis and psoriasis with implications for treatment. Exp Dermatol 2018;27:409–17.

Hijnen D, De Bruin-Weller M, Oosting B, Lebre C, De Jong E, Bruijnzeel-Koomen C, et al. Serum thymus and activation-regulated chemokine (TARC) and cutaneous T cell- attracting chemokine (CTACK) levels in allergic diseases: TARC and CTACK are disease-specific markers for atopic dermatitis. J Allergy Clin Immunol 2004;113:334–40.

Ip WK, Wong CK, Li ML, Li PW, Cheung PF, Lam CW. Interleukin-31 induces cytokine and chemokine production from human bronchial epithelial cells through activation of mitogen-activated protein kinase signalling pathways: implications for the allergic response. Immunology 2007;122:532–41.

Jahnz-Rozyk K, Targowski T, Paluchowska E, Owczarek W, Kucharczyk A. Serum thymus and activation-regulated chemokine, macrophage-derived chemokine and eotaxin as markers of severity of atopic dermatitis. Allergy 2005;60:685–8.

Kakinuma T, Nakamura K, Wakugawa M, Mitsui H, Tada Y, Saeki H, et al. Thymus and activation-regulated chemokine in atopic dermatitis: serum thymus and activation-regulated chemokine level is closely related with disease activity. J Allergy Clin Immunol 2001;107:535–41.

Keren A, Reich K, Bertolini M, Moga A, Riethmüller C, Ullmann Y, et al. Autologous Th2-polarized lymphocytes induce atopic dermatitis lesions in non-atopic human skin xenotransplants. Allergy 2023;78:1538–53.

Kishi R, Toyama S, Tominaga M, Kamata Y, Komiya E, Kaneko T, et al. Effects of dupilumab on itch-related events in atopic dermatitis: implications for assessing treatment efficacy in clinical practice. Cells 2023;12:239.

Lytvyn Y, Gooderham M. Targeting interleukin 13 for the treatment of atopic dermatitis. Pharmaceutics 2023;15:568.

McCormick SM, Heller NM. Commentary: il-4 and IL-13 receptors and signaling. Cytokine 2015;75:38–50.

Moyle M, Cevikbas F, Harden JL, Guttman-Yassky E. Understanding the immune landscape in atopic dermatitis: the era of biologics and emerging therapeutic approaches. Exp Dermatol 2019;28:756–68.

Reich K, Thyssen JP, Blauvelt A, Eyerich K, Soong W, Rice ZP, et al. Efficacy and safety of abrocitinib versus dupilumab in adults with moderate-to-severe atopic dermatitis: a randomised, double-blind, multicentre phase 3 trial. Lancet 2022;400:273–82.

Ruzicka T, Hanifin JM, Furue M, Pulka G, Mlynarczyk I, Wollenberg A, et al. Anti-interleukin-31 receptor A antibody for atopic dermatitis. N Engl J Med 2017;376:826–35.

Silva JP, Vetterlein O, Jose J, Peters S, Kirby H. The S228P mutation prevents in vivo and in vitro IgG4 Fab-arm exchange as demonstrated using a combination of novel quantitative immunoassays and physiological matrix preparation. J Biol Chem 2015;290:5462–9.

Silverberg JI, Pinter A, Pulka G, Poulin Y, Bouaziz JD, Wollenberg A, et al. Phase 2B randomized study of nemolizumab in adults with moderate-to-severe atopic dermatitis and severe pruritus. J Allergy Clin Immunol 2020;145:173–82.

Simpson EL, Bieber T, Guttman-Yassky E, Beck LA, Blauvelt A, Cork MJ, et al. Two phase 3 trials of dupilumab versus placebo in atopic dermatitis. N Engl J Med 2016;375:2335–48.

Ständer S, Yosipovitch G, Legat FJ, Lacour JP, Paul C, Narbutt J, et al. Trial of nemolizumab in moderate-to-severe prurigo nodularis. N Engl J Med 2020;382:706–16.

Takamori A, Nambu A, Sato K, Yamaguchi S, Matsuda K, Numata T, et al. IL-31 is crucial for induction of pruritus, but not inflammation, in contact hypersensitivity. Sci Rep 2018;8:6639.

Tazawa T, Sugiura H, Sugiura Y, Uehara M. Relative importance of IL-4 and IL-13 in lesional skin of atopic dermatitis. Arch Dermatol Res 2004;295:459–64.

Trier AM, Kim BS. Cytokine modulation of atopic itch. Curr Opin Immunol 2018;54:7–12.

Tsoi LC, Rodriguez E, Degenhardt F, Baurecht H, Wehkamp U, Volks N, et al. Atopic dermatitis is an IL-13-dominant disease with greater molecular heterogeneity compared to psoriasis. J Invest Dermatol 2019;139:1480–9.

Wahlgren CF. Itch and atopic dermatitis: an overview. J Dermatol 1999;26:770–9.

Werfel T, Allam JP, Biedermann T, Eyerich K, Gilles S, Guttman-Yassky E, et al. Cellular and molecular immunologic mechanisms in patients with atopic dermatitis. J Allergy Clin Immunol 2016;138:336–49.

Yamamoto S, Kobayashi I, Tsuji K, Nishi N, Muro E, Miyazaki M, et al. Upregulation of interleukin-4 receptor by interferon-gamma: enhanced

interleukin-4-induced eotaxin-3 production in airway epithelium. Am J Respir Cell Mol Biol 2004;31:456–62.

Yu G, Wang LG, Yan GR, He QY. DOSE: an R/Bioconductor package for disease ontology semantic and enrichment analysis. Bioinformatics 2015;31:608–9.

Zhang Y, Jing D, Cheng J, Chen X, Shen M, Liu H. The efficacy and safety of IL-13 inhibitors in atopic dermatitis: A systematic review and meta-analysis. Front Immunol 2022;13:923362.

Zhao J, Jiang L, Deng L, Xu W, Cao Y, Chen C, et al. Important roles of CD32 in promoting suppression of IL-4 induced immune responses by a novel anti-IL-4Rα therapeutic antibody. mAbs 2019;11:837–47.

This work is licensed under a Creative Commons Attribution-NonCommercial-NoDerivatives 4.0 International License. To view a copy of this license, visit http://creativecommons.org/licenses/by-nc-nd/4.0/